Nuclear Physics B198 (1982) 13–25

CROSS SECTIONS AT "ASYMPTOTIC" ENERGIES IN THE $\bar{p}p$ COLLIDER

J. BAUMEL, M. FEINGOLD and M. MOSHE

Department of Physics, Technion-Israel Institute of Technology, Haifa 32000, Israel

Received 2 July 1981

As a whole new range of energies will be soon experimentally studied, we present predictions for hadronic cross sections at future very high energy accelerators. All calculations are based on results accumulated in reggeon field theory, where methods of field theory (in the continuum and on the lattice) and statistical mechanics have been used. We have employed these results and translated them into a manageable phenomenological analysis of existing FERMILAB-ISR data. The size of the non-leading terms is determined and enables us to predict cross sections at energies in the range of the near future $\bar{p}p$ collider. Parameter-free scaling functions and critical exponents which are exactly calculable in RFT are thus brought to an experimental test.

1. Introduction

In the very near future, particle scattering data at energies up to 540 GeV in the center of mass will be reached in the SPS $\bar{p}p$ collider. Particle scattering will be measured in an entirely new regime of energies and several interesting questions will hopefully be answered (finding traces of the intermediate vector bosons, jet phenomena and the behavior of σ_{tot} and σ_{el} at very high energies, etc. [1]). Present understanding of the theory of strong interactions (QCD) is unfortunately insufficient to give unambiguously derived detailed predictions for the main bulk of soft process data. Indeed, calculating a proton-proton cross section, starting from the QCD underlying theory, is still a formidable task. Analogously, one can easily find examples of measurable quantities in atomic and solid state physics impossible to calculate starting from the underlying QED lagrangian. In no way would this imply a deficiency in the theories, but rather that, in some problems, the degrees of freedom for describing the phenomena have to be properly chosen, and in many cases, they may be entirely different from the quanta of the fundamental theory. Thus, quarks and gluon fields are perfect for calculating many observables in strong interaction physics, certainly in processes dominated by the short-distance behavior of the theory. But it has been repeatedly suggested that different degrees of freedom are necessary for soft processes. These collective degrees of freedom are built in a complex manner [2] out of the fundamental fields of the theory resembling the

construction of phonons and spin waves from the more fundamental lattice site variables.

Reggeon field theory (RFT) long ago provided detailed predictions for scattering amplitudes at very high energies [3a]*,**. Methods of field theory and statistical mechanics had been used to perform very detailed calculations of the critical behavior of the pomeron singularity. This activity, almost extinct today, had provided unique, unambiguous results in the form of scaling functions [5] and critical exponents [6,7] analogously to the detailed calculations of any typical statistical mechanics problem near a phase transition [3,4,7,9]***. Though interesting work is still being carried out in an attempt to derive the RFT from the underlying strong interaction theory [2], the work aimed at sharpening the theory's predictions had come to a stand-still for several reasons. Among them is the fact that the theory had almost never been able to predict at what energies scaling behavior will set in. This question is still open and is left for the experimentalists to answer.

In the past, the theoretical attitude employed in this field had been based on the feeling that only at high energies above the ISR regime can one hope that the results will be of practical use. This explains the lack of almost any phenomenological work in relation to RFT. Thus, many of the theory's predictions were left in a very rough state, such as the asymptotic expansion of the n-point Green function for the pomeron field, $\varepsilon = 4 - D$ expanded scaling functions, and the high-temperature expansion for the lattice theory in dimension $D = 1$ and 2.

As the operation of the SPS collider is approaching, we felt that it may be useful to bring some of the theory's predictions to a state that can be confronted with the data. We especially treated and emphasized the predictions of the approach to asymptotic scaling of the cross sections. At very high energy the approach to scaling is governed in RFT by a well-defined functional form that had been calculated in the past [10].

The plan of this work was to carry out a study, which though suggested a long time ago [11], seemed, at that time, to be lacking any appeal since the SPS collider as well as any other very high energy accelerator were still only plans for the far future. It was suggested to use the ISR energy regime data in order to extract the free parameters that determine the strength of both the leading term and non-leading approach to scaling terms. Using the fit at these low energies, one determines the parameters of the scaling Green functions describing the cross sections at much higher energies, namely, in the SPS $\bar{p}p$ collider regime.

In sects. 2 and 3 we present the predictions for the total cross section summarized in figs. 2a, b and 3. The predictions for the shape of the diffraction peak, the first

* For order ε^2 calculations see [3b].

** For reviews on RFT see ref. [4].

*** In ref. [7], a very detailed high-temperature expansion up to 10th and 21st orders had been performed. This model has been recently shown [8] to be in the same universality class of an interesting statistical mechanics problem (directed bond percolation [DBP]).

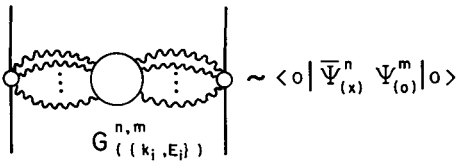

Fig. 1. The n incoming, m outgoing pomeron Green functions whose asymptotic behavior determine the hadronic cross sections at high energies.

minimum and the second maximum location are summarized in figs. 6–8. We leave the more technical details for the appendix.

2. Total cross section for pp and $\bar{p}p$

The total hadron-hadron cross section at high energy has been calculated in RFT from the pomeron $G^{n,m}(k_i, E_i)$ Green functions (fig. 1). It has the asymptotic large-s behavior

$$\sigma_T^{\text{asymp}}(s) = \beta_0(\ln s)^{\eta}\left[1 + \beta_1(\ln s)^{-\lambda} + \beta_2(\ln s)^{-1-\eta}\right], \tag{1}$$

where we take the scale of s to be 1 GeV^2. The exponent η and the approach to scaling exponent λ (λ is equal to the derivative of the beta function at the fixed point [10]) are known to a very good accuracy from the RFT on the lattice calculations [7]* (the reggeon quantum spin model) as well as the high order behavior of perturbation [6, 8, 9] theory; $\eta = 0.26 \pm 0.02$, $\lambda = 0.49 \pm 0.01$. β_i are not calculable by the theory. We also added two terms to σ_T^{asymp}:

$$\sigma_T(s) = \sigma_T^{\text{asymp}}(s) + \beta_0\left(\beta_3 s^{-1/2} + \beta_4 s^{-1}\right) \tag{2}$$

as low-energy remnants coming presumably from possible lower trajectories**. The powers $-\frac{1}{2}$ and -1 can be freely changed around these values without much change of our final results.

The coefficients β_0 and β_1 are related to the coupling of the one-particle irreducible Green function $G^{1,1}(k, E)$ of the pomeron to the particle line; thus, in fitting the Fermilab-ISR data we demanded $\beta_0 = \bar{\beta}_0$ and $\beta_1 = \bar{\beta}_1$, where $\bar{\beta}_0$ and $\bar{\beta}_1$ are the corresponding coefficients used for the $\bar{p}p$ data. The parameters $\bar{\beta}_2$, $\bar{\beta}_3$ and $\bar{\beta}_4$ were free to vary and obtain values different from β_2, β_3 and β_4 in the pp data. The

* The approach to scaling exponent has also been calculated in DBP and shown to be the same as λ in RFT [eq. (1)], see ref. [9].

** Abarbanel and Sugar [12] calculated the logarithmic correction to a typical term in eq. (2) due to pomeron interactions. Their result to first order in ε was $s^{-\alpha_R}(\ln s)^{\gamma}$, where $\gamma = \frac{1}{12}$. γ is too small to be significant in the present phenomenological analysis.

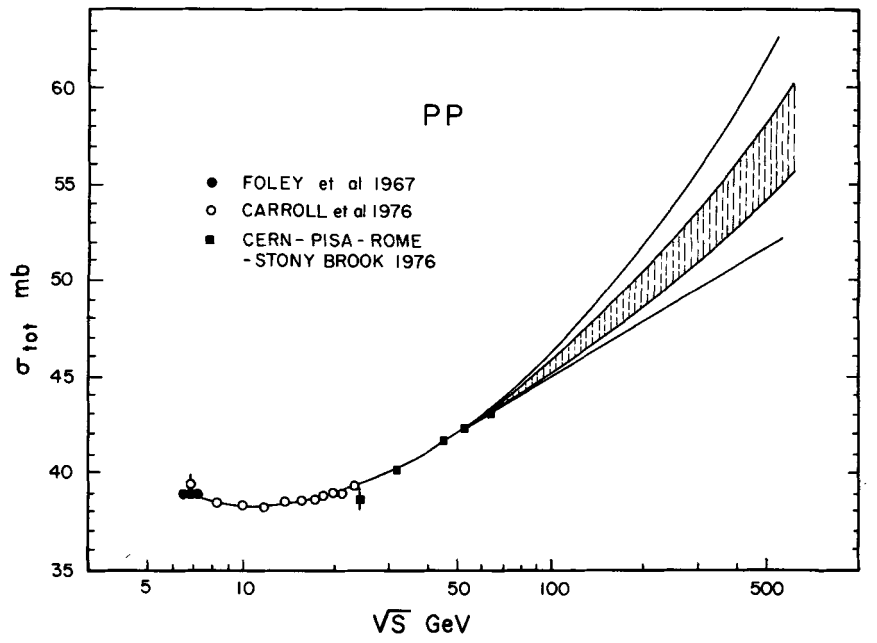

(a)

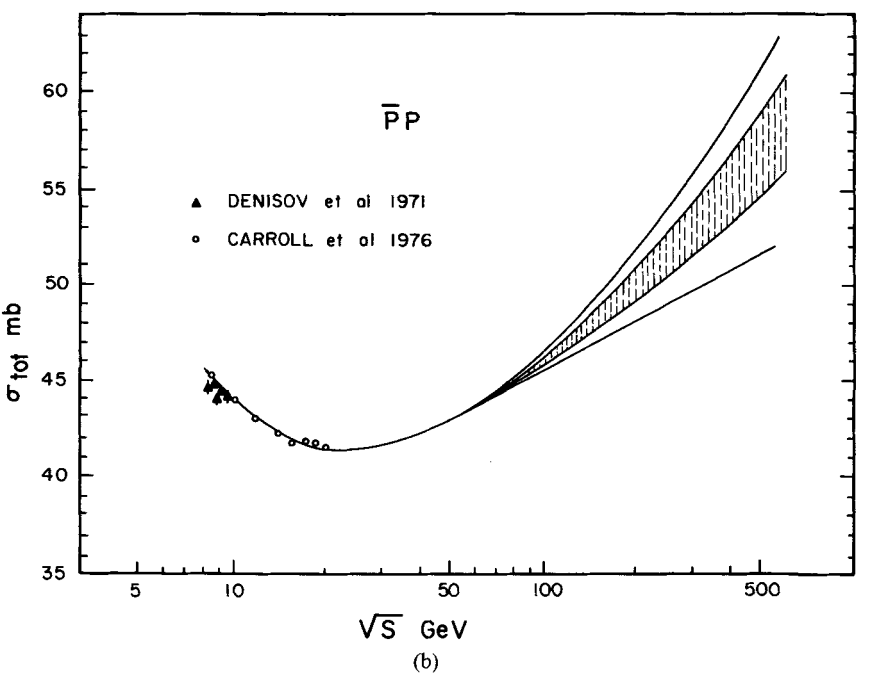

(b)

Fig. 2. (a) Predictions for the proton-proton cross sections at very high energies. Also shown is the lower energy data (Fermilab-ISR) fitted with eqs. (1), (2). The shadowed area corresponds to the better χ^2 values (see appendix). (b) Same as (a) here for $\bar{p}p$. The shadowed area corresponds to the shadowed area fits of (a).

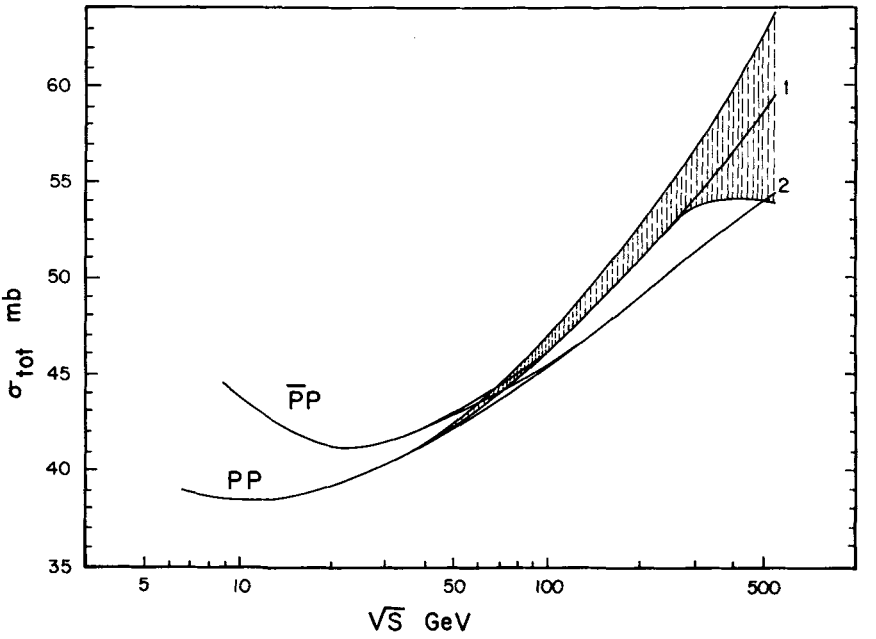

Fig. 3. Comparison of our predictions (between lines 1 and 2) and the results of ref. [14] (shadowed area).

asymptotic relation $\sigma^{\bar{p}p}(s) = \sigma^{pp}(s)$, a natural result of RFT, is built into the fit and allows us to learn about $\sigma^{\bar{p}p}$ from σ^{pp} at high s.

We have used the data of ref. [13] for the pp and $\bar{p}p$ total cross section and the results of our calculations and predictions are shown in figs. 2a, b. We also compared in fig. 3 our calculations to those of ref. [14], where the increase of the total cross section is predicted, using the measured real part of the proton-proton elastic amplitude from the Coulomb interference experiment. Our best χ^2 predicted cross section in the high-s regime is somewhat lower than in ref. [14]. We have not used the cosmic ray data of ref. [15] in our fit; it tends to fall only slightly above our predicted $\sigma_T(s)$. Its quoted errors are too large to reach a definite conclusion and future $\bar{p}p$ collider data are certainly much awaited here. The predicted values for β_i as well as other details on the results in figs. 2a, b and 3 are given in the appendix.

3. Elastic cross section and the diffraction structure

The elastic cross section for hadron-hadron scattering can be calculated from the scaling form of the pomeron Green function (fig. 1) in a manner similar to the way in which $\sigma_T(s)$ was calculated. It has the form [5,10]:

$$\frac{d\sigma}{dt} = \beta^4(t)(\ln s)^{2\eta} F_0\big(ct(\ln s)^z\big)\big\{1 + F_1\big(ct(\ln s)^z\big)\cdot(\ln s)^{-\lambda} + \cdots\big\}. \qquad (3)$$

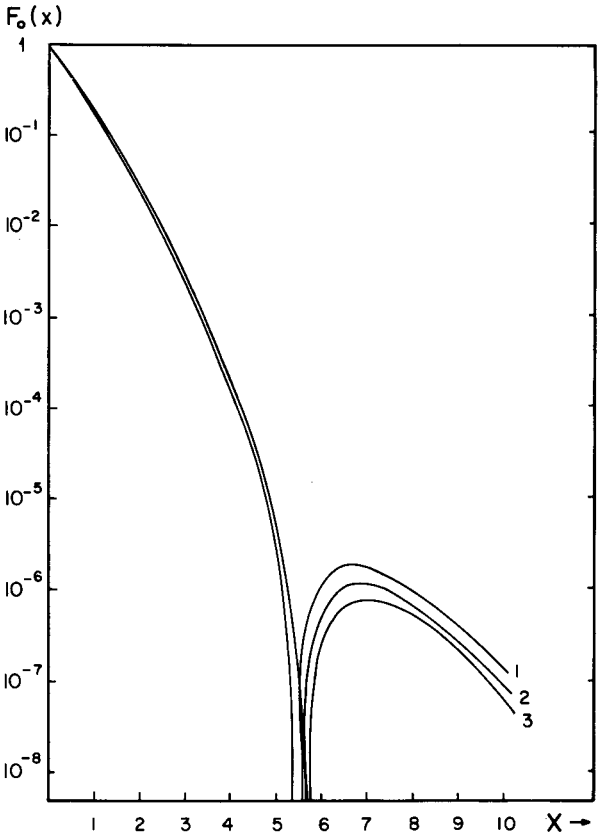

Fig. 4. The scaling function $F_0(x)$ of eq. (3) normalized to $F_0 = 1$ for different values of δ (see appendix) ($\delta = 5 \cdot 10^{-2}$, 10^{-2}, $5 \cdot 10^{-3}$ for lines, 1, 2, 3, respectively).

The leading term scaling function, $F_0(x)$, is, in principle, parameter free and exactly calculable in RFT. However, when expressed as a function of t, the scale of t is, of course, a parameter. $F_0(x)$ has been calculated [16] up to order ε^2. It shows the same general interesting behavior as the $O(\varepsilon)$ calculation [5] at low t up to the second maximum*. The exponent z has been calculated in refs. [3, 6, 7]; $z = 1.13 \pm 0.01$. $\beta(t)$ has a typical exponential behavior and is not calculable by the theory. There is no $O(\varepsilon^2)$ calculation of $F_1(ct(\ln s)^z)$, but its value at $t = 0$ is related to the coefficient β_1 in $\sigma_T(s)$ and, therefore, certainly is not negligible; neither are there any calculations of even lower order terms in eq. (3). We will concentrate on the forward diffractive peak, the first minimum and second maximum, a region where, as mentioned above, $O(\varepsilon)$ and $O(\varepsilon^2)$ calculations do not differ much, and since we are interested mainly in the approach to scaling, we will use the $O(\varepsilon)$ expression for $F_0(x)$ and fit $(\ln s)^{-\lambda} F_1(x)$ from the ISR data. The expression for $F_0(x)$ is given by a principal

* Note that refs. [5, 16] use different numerical techniques for performing the integrations.

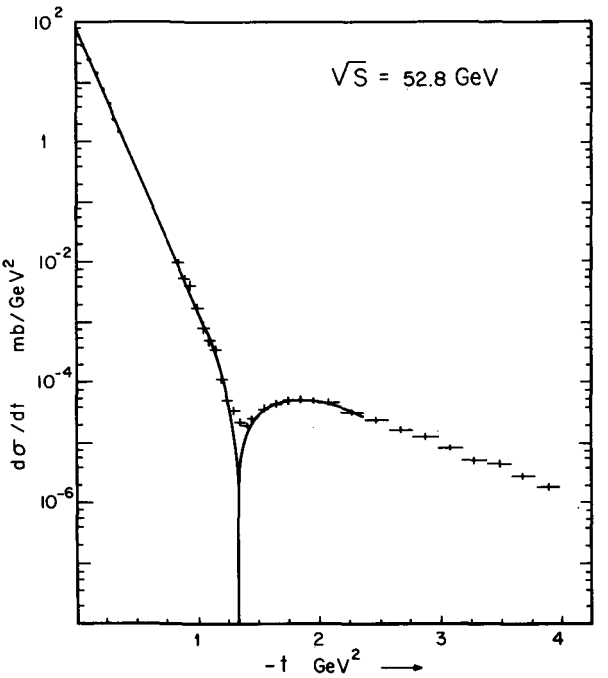

Fig. 5. ISR data ($\sqrt{s} = 52.8$ GeV) as described by the asymptotic scaling function and the approach to scaling, non-leading term in eq. (3).

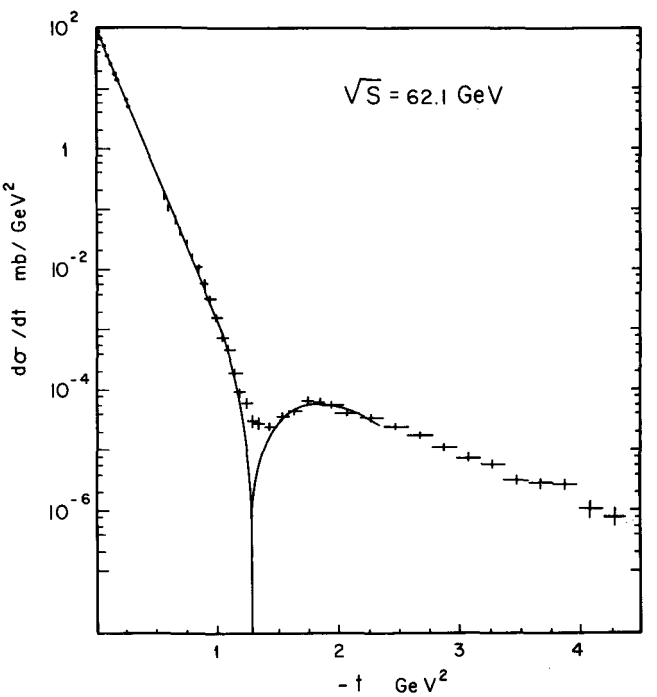

Fig. 6. Same as in fig. 5 at $\sqrt{s} = 62.1$ GeV.

part integral [5] in the appendix, where we also explain some technical details about the end-point behavior of this integrand, leaving some freedom in the expression of $F_0(x)$ seen in fig. 4. The ISR data [17] is well described by eq. (3), as seen in figs. 5 and 6. This fit determines all our free parameters. We are then able to predict the shape of the elastic cross section in fig. 7 and the location of the first minimum and the second maximum in fig. 8. At $\sqrt{s} \simeq 500$ GeV we find that the elastic cross section is mostly dominated by $F_0(x)$ and thus our predictions are for pp as well as for $\bar{p}p$ data at this energy. Indeed, we found out that using the new data [18] on $\bar{p}p$ leads us to the same "asymptotic" elastic cross section as in fig. 7.

To summarize, the early appearance of the equality of the total cross sections and the similarity of the diffraction peak in pp and $\bar{p}p$ is a remarkable fact which may indicate that the essential feature of the asymptotic RFT results shows up already at the top ISR energies. The presently performed experiments, and those planned for the near future with $\bar{p}p$ beams at the ISR and in the SPS collider, will hopefully further confirm that we are indeed in the "asymptotic" energy regime. One should note, however, the following two facts that have to be seriously considered in relation to the predicted asymptotic t dependence in RFT: (a) The above mentioned difficulty with the end point of the integration region, which is explained in some

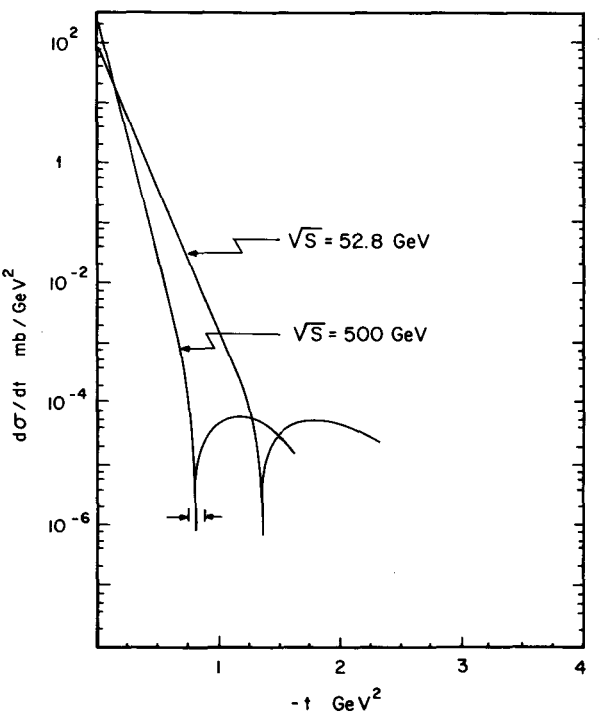

Fig. 7. Prediction for the elastic cross section at $\sqrt{s} = 500$ GeV, using the fitted parameters from the ISR regime.

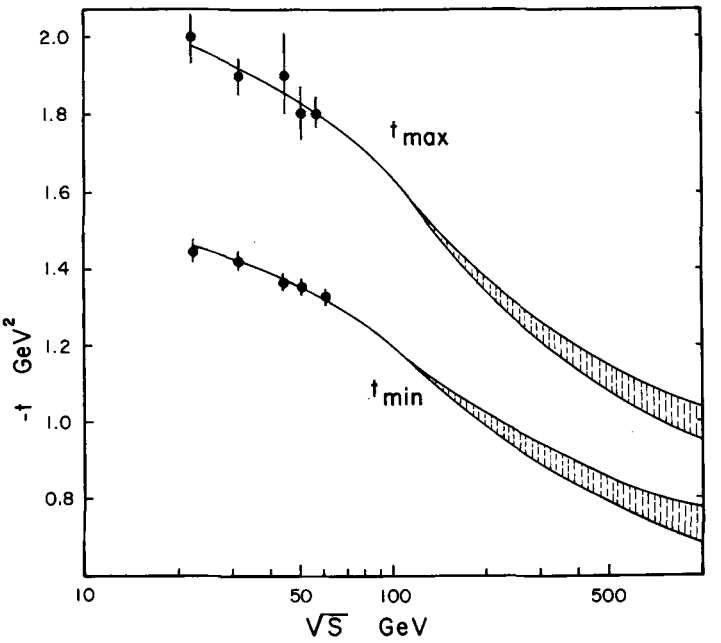

Fig. 8. Predictions for the location of the first minimum and the second maximum as a function of s. Data are from ref. [17].

detail in appendix A.2. (b) In the asymptotic RFT predictions there is no t-dependent signature factor and the effect of its real part is viewed as a subasymptotic term (in the phase-transition nomenclature these terms in the lagrangian would be called "irrelevant"). In practice, one does not know for sure whether such a real part could be significant at the t values at which the dip structure is predicted from the leading RFT terms.

Appendix

In this appendix we will present some details of calculations involved in reaching the fits and predictions in figs. 2a, 2b, 7 and 8.

A.1. TOTAL CROSS SECTION

For the pp total cross section we have chosen the most precise data points at each given energy from ref. [13]. Altogether we used 17 data points, shown in fig. 2a. With eqs. (1) and (2) we get a χ^2 of 9–11 for 12 degrees of freedom in our best fits, and thus find β_0 and β_i ($i = 1$–4). The values of $\sigma_T(s)$ for the range of parameters that

gave $\chi^2 = 9$–11 for 12 DOF, lie in the shadowed area in fig. 2a. A typical fit in this region is*

$$\beta_0 = 90 \pm 2, \qquad \beta_1 = -3.32 \pm 0.06, \qquad \beta_2 = 6.72 \pm 0.10,$$

$$\beta_3 = -1.41 \pm 0.02, \qquad \beta_4 = -4.34 \pm 0.08. \tag{A.1}$$

In general, each individual value of β_i tends to vary in a much wider range of values than those in eq. (A.1), (as seen in fig. 2a), giving different minima of χ^2 within the range of $9 \leqslant \chi^2 \leqslant 11$. We also present in fig. 2a the range of values of $\sigma_T(s)$, if we allow χ^2 to vary up to $\chi^2 = 17$ (for 12 DOF). These values are included between the outer lines in fig. 2a.

Using the values of β_0 and β_1 for each fitted σ_T^{pp}, we then fitted the $\bar{p}p$ data with the three parameters $\bar{\beta}_i (i = 2$–$4)$ in eqs. (1), (2). In most cases the fitted $\bar{\beta}_2$ in $\bar{p}p$ data came out to lie very close to β_2 from the pp data, whereas the "low energy" parameters, $\{\bar{\beta}_3, \bar{\beta}_4\}$ and $\{\beta_3, \beta_4\}$, are different. This can be well understood within RFT and is of no surprise, as could be guessed from looking at the steeper decrease in the $\bar{p}p$ data. We used altogether 8 data points of Carroll et al. in ref. [13], which have the smallest error, and found $\chi^2 \simeq 7.8$–8.8 for 5 degrees of freedom. The predicted $\bar{p}p$ total cross section in the shadowed area and between the outer lines in fig. 2b correspond to fits with the same β_0, β_1 that lie in the shadowed area and outer lines of fig. 2a. Thus, for example, the typical fit in eq. (A.1) for pp produced for $\bar{p}p$ a fit

$$\bar{\beta}_0 = 90, \qquad \bar{\beta}_1 = -3.32, \qquad \text{(input)},$$

$$\bar{\beta}_2 = 6.70 \pm 0.10, \qquad \bar{\beta}_3 = -0.92 \pm 0.04, \qquad \bar{\beta}_4 = -3.1 \pm 0.1. \tag{A.2}$$

For the asymptotic predictions in fig. 3 we used only the best χ^2 range and compared our predictions to ref. [14].

* Cardy and Moshe [19] have shown that due to the renormalization of the n-pomeron–particle vertex as a composite operator in RFT, each multi-pomeron Green function is a sum of scaling terms that include the leading $G^{1,1} \sim (\ln s)^{\eta}$ term. Thus, the approach to scaling will be governed by terms like $(\ln s)^{\eta - \lambda}$ given in eq. (1) and a lower term of the form $(\ln s)^{\eta - 2\lambda}$. It has been also shown that irrelevant operators (e.g., $\bar{\psi}^2 \psi^2$) will introduce terms of the form $(\ln s)^{-1+O(\varepsilon)}$. Numerically $-\eta + 2\lambda = -0.26 + 2 \times 0.49$ is close to one and certainly $(\ln s)^{\eta - 2\lambda}$ cannot be distinguished phenomenologically from $(\ln s)^{-1+O(\varepsilon)}$; thus we took in the fit of eq. (1) only the $(\ln s)^{-1}$ term to represent both. The coefficient of this term is β_2 in eq. (1) and eq. (A.1).

A.2. ELASTIC CROSS SECTION

The expression for the elastic cross section calculated in RFT is given in eq. (3). The scaling function, $F_0(x) = \Phi_1^2(x)$, is given by Abarbanel et al. in ref. [5]:

$$\Phi_1(x) = 0.8639x^{-2/13}\cos(0.4833 - 0.2702x^{12/13})\exp(-1.062x^{12/13})$$

$$-0.1519x^{-2/13}\mathrm{P}\int_0^1 \mathrm{d}z \frac{\psi(x,z)}{13z-7}, \tag{A.3}$$

where

$$\psi(x,z) = \frac{13z-1}{z^{15/13}(1-z)^{11/13}}\sin\left(0.4833 - \frac{0.12621x^{12/13}}{z^{1/13}(1-z)^{12/13}}\right)$$

$$\times\exp\left(-\frac{0.5121x^{12/13}}{z^{1/13}(1-z)^{12/13}}\right). \tag{A.4}$$

In order to integrate the principal value integral on the computer we used

$$\mathrm{P}\int_0^1 \frac{\psi(x,z)}{13z-7}\,\mathrm{d}z = \int_0^1 \left[\frac{\psi(x,z)-\psi(x,\frac{7}{13})}{13z-7}\right]\mathrm{d}z + \psi(x,\tfrac{7}{13})\cdot\frac{\ln(\frac{6}{7})}{13}. \tag{A.5}$$

The result for $F_0(x) = \Phi_1^2(x)$ normalized to $F_0(0) = 1$ is shown in fig. 4. Notice, however, the very rapid oscillatory nature of the integrand as $z \to 0$. For example, at $x = 4$ we have:

$$\psi_{(4,z)} \underset{z\to 0}{\to} z^{-15/13}\sin\left(0.4833 - \frac{0.4538}{z^{1/13}}\right)\exp\left(-\frac{1.8412}{z^{1/13}}\right). \tag{A.6}$$

Though, indeed, $\psi_{(x,z)} \to 0$ as $z \to 0$ and is integrable, it oscillates wildly in the very low z region ($z < 10^{-2}$–10^{-3}). Physically, this region corresponds to large $E = 1 - j$ values in the complex angular momentum plane [5]. In this regime the whole calculation is unreliable; our knowledge of $G^{n,m}(k, E)$ is mostly in the $E \to 0$ region. We thus put a cut-off at the lower region of integration and changed 0 to $\delta \simeq \mathrm{O}(10^{-2}$–$10^{-3})$ in eq. (A.3). The final result depends slightly on δ, within this range, and is shown in fig. 4. Though not specified there, we found that in ref. [5] $\delta = 10^{-2}$. As mentioned above, in the low-t region, up to the second maximum, the

results of ref. [16] ($O(\varepsilon^2)$) are very close to those of ref. (5) ($O(\varepsilon)$). Relying on this stability, we conclude that the asymptotic $\Phi_1(x)$ is described to a very good approximation by eq. (A.3). In fitting $\sigma_T(s)$ in the ISR regime only, the first two terms in eq. (1) suffice, thus we do not have to use additional non-leading terms to those already specified in eq. (3) in fitting $d\sigma/dt$ at the ISR energies.

We used the data in ref. [17]; figs. 5 and 6 show our fit [eq. (3)] with $\beta^4(t) \sim e^{3.5t}$, and $F_0(x)$ from fig. 4. The scale for t is also fitted:

$$x = ct(\ln s)^z = 0.398t(\ln s)^{1.13}. \tag{A.7}$$

We are then able to predict $d\sigma/dt$ at higher energies. This is shown in fig. 7. The uncertainty as shown at the bottom of the graph with $\sqrt{s} = 500$ GeV is an indication of the error involved. It has its origin in the dependence of our results on choosing δ, as shown in fig. 4. We regard this as an uncertainty due to low energy components, namely, lower trajectories contributing to $G^{1,1}(k, E)$ at large $E = 1 - j$.

In fig. 8 we show our predictions for the location of the minimum ($t_{min}(s)$) and the second maximum ($t_{max}(s)$) in the elastic cross section. The data are from ref. [17]. We also notice that the data of ref. [18] for $\bar{p}p$ are well described by our fit to the pp data; the significance of this has been discussed in sect. 3.

References

[1] M. Jacob, Physics at collider energy, Talk at 1980 CERN School of Physics, Malente, Germany, June, 1980
[2] A.R. White, CERN preprints TH.2976 (1980), TH.3058 (1981); Proc. 2nd Int. Symp. on Hadron structure, Kazimierz, Poland (1979);
J. Bartels, Nucl. Phys. B151 (1979) 293; B175 (1980) 365
[3] (a) H.D.I. Abarbanel and J.B. Bronzan, Phys. Rev. D9 (1974) 2397;
A.A. Migdal, A.M. Polyakov and K.A. Ter-Martirosyan, ZhETF (USSR) 67 (1974) 84
(b) J.B. Bronzan and J.W. Dash, Phys. Rev. D10 (1974) 4208 (E:D12 (1974) 1850);
M. Baker, Nucl. Phys. B80 (1974) 62 (E:B85 (1975) 545, B100 (1975) 411)
[4] H.D.I. Abarbanel, J.B. Bronzan, R.L. Sugar and A.R. White, Phys. Reports 21 (1975) 119;
M. Moshe, Phys. Reports 37 (1978) 255
[5] H.D.I. Abarbanel, J. Bartels, J.B. Bronzan and D. Sidhu, Phys. Rev. D12 (1975) 2459, 2799;
W.R. Frazer and M. Moshe, Phys. Rev. D12 (1975) 2370;
W.R. Frazer, J.R. Fulco, H.J. Hoffman and R.L. Sugar, Phys. Rev. D14 (1976) 2387
[6] J.L. Cardy, Phys. Lett. 67B (1977) 97
[7] R.C. Brower, M.A. Furman and M. Moshe, Phys. Lett. 76B (1978) 213
[8] J.L. Cardy and R.L. Sugar, J. Phys. A13 (1980) L423
[9] J. Adler, M. Moshe and V. Privman, J. Phys. A14 (1981) L363
[10] W.R. Frazer and M. Moshe, Phys. Lett. 57B (1975) 475
[11] M. Moshe and A.R. White, CERN preprint (Sept., 1977); Summary of two talks at Workshop on future ISR physics, CERN, Geneva;
M. Jacob, CERN Report ISR Workshop/2-10 (1977).
[12] H.D.I. Abarbanel and R.L. Sugar, Phys. Rev. D10 (1974) 721

[13] G. Bellettini et al., Phys. Lett. 14 (1965) 164;
W. Galbraith et al., Phys. Rev. 138B (1965) 913;
K.J. Foley et al., Phys. Rev. Lett. 19 (1967) 857;
S.P. Denisov et al., Phys. Lett. 36B (1971) 528;
U. Amaldi et al., Phys. Lett. 43B (1973) 231;
U. Amaldi et al., Phys. Lett. 44B (1973) 112;
S.R. Amendolia et al., Nuovo Cim. 17A (1973) 735;
K. Eggert et al., Nucl. Phys. B98 (1975) 93;
A.S. Carroll et al., Phys. Lett. 61B (1976) 303;
CERN-Pisa-Rome-Stony Brook Collaboration, Phys. Lett. 62B (1976) 460;
U. Amaldi et al., Phys. Lett. 66B (1977) 390
[14] U. Amaldi et al., Phys. Lett. 66B (1977) 390
[15] G.B. Yodh, Y. Pal and J.S. Trefil, Phys. Rev. Lett. 28 (1972) 1005; Phys. Rev. D8 (1973) 3233;
V. Barger, F. Halzen, T.K. Gaisser, C.J. Noble and G.B. Yodh, Phys. Rev. Lett. 17 (1974) 1051;
G.B. Yodh, Maryland preprint no. 78-004, Technical Report, (April, 1977), and references therein
[16] J.W. Dash and T. Grandou, Z. Phys. C3 (1979) 9;
J.W. Dash and C. Bourrely, Marseilles preprint CPT-81/P.1280 (1981)
[17] M. Holder et al., Phys. Lett. 35B (1971) 355; 36B (1971) 400;
G. Barbiellini et al., Phys. Lett. 39B (1972) 663;
U. Amaldi et al., Phys. Lett. 36B (1971) 504; 43B (1974) 231;
A. Böhm et al., Phys. Lett. 49B (1974) 491;
N. Kwak et al., Phys. Lett. 58B (1975) 233;
E. Nagy et al., Nucl. Phys. B150 (1979) 221;
U. Amaldi and K.R. Schubert, Nucl. Phys. B166 (1980) 301
[18] Z. Asa'd et al., Annecy-CERN-Copenhagen-Genova-Oslo-London Collaboration, Proc. 20th Int. Conf. on High-energy physics, Madison, July, 1980
[19] J.L. Cardy and M. Moshe, Nucl. Phys. B139 (1978) 291